Environ Health Perspect

DOI: 10.1289/EHP2877

Supplemental Material

Metabolic Effects of a Chronic Dietary Exposure to a Low-Dose Pesticide Cocktail in Mice: Sexual Dimorphism and Role of the Constitutive Androstane Receptor

Céline Lukowicz, Sandrine Ellero-Simatos, Marion Régnier, Arnaud Polizzi, Frédéric Lasserre, Alexandra Montagner, Yannick Lippi, Emilien L. Jamin, Jean-François Martin, Claire Naylies, Cécile Canlet, Laurent Debrauwer, Justine Bertrand-Michel, Talal Al Saati, Vassilia Théodorou, Nicolas Loiseau, Laïla Mselli-Lakhal, Hervé Guillou, and Laurence Gamet-Payrastre

Table of Contents

Figure S5. Body weight of WT males (**A**) fed control and pesticide chow and of females (**B**) fed control and pesticide chow after 16, 36 and 48 weeks of exposure. Results are the mean ± standard error of the mean with n=5 (cages 1 and 2) and n=4 (cages 3 and 4).

Figure S6. Blood glucose and blood insulin measured in WT male (**A**) and female (**B**) mice after 52 weeks of control (C) or pesticide (P) chow. Data are presented as mean ± standard error of the mean. n= 18 mice per group.

Figure S7. Analysis of plasma from WT male (**A, B**) and female (**C**, **D**) mice fed control (C) or pesticide (P) for 52 weeks. Data are presented as the mean ± standard error of the mean. *P<0.05 **P<0.01 ***P<0.001. P-values represent the difference between mice fed control chow and those fed pesticide chow as determined using a Student's t-test; n=18 mice per group. FFA, free fatty acid; TG, triglyceride; LDL, low density lipoprotein; HDL, high density lipoprotein.

Figure S8. O-PLS-DA score plots derived from the plasma spectra of WT males (**A**), WT females (**B**), CAR-/- males (**C**) and CAR-/- females (**D**) after 48 weeks of either control (C) or pesticide (P) chow. Plasmatic biomarkers of pesticide exposure were investigated using ^{1}H-NMR based metabolomics.Q2Y represents the goodness of fit for the PLS-DA models and p-values were derived using 1000 permutations of the Y matrix.

Figure S9. Hepatic lipid analysis of WT male (M) and female (F) mice after 52 weeks of eating either control (C) or pesticide (P) chow. (**A**) Heat map with hierarchical clustering, allowing the definition of 6 lipid clusters, as labeled on the left side of the map. (**B**) The relative PS32:0, PS34:0, PS36:1 abundances for cluster 5 (lipid species specifically down-regulated in males exposed to pesticides. (**C**) The relative SM18:1/16:0, PC30:0, PC 32:0 abundances for cluster 4 (lipid species up-regulated in males and females exposed to pesticides). (**D**) The relative C18:2n-6, Cerd18:1/C26:1, SM18:1/24:1 abundances for cluster 2 (lipid species down-regulated in males and females exposed to pesticides). (**E**) The relative TG51, TG53, PI36:0 abundances for cluster 1 (lipid species specifically up-regulated either in males or in females exposed to pesticides). Data are presented as the mean of relative abundance in each lipid species ± standard error of the mean. * P<0.05, ** P<0.01, *** P<0.001. P-values represent the difference between mice fed control chow and those fed pesticide chow as determined using a Student's t-test; n=18 mice per group. PS, Phosphatidylserin; SM Sphingomyelin; PC, Phosphatidlcholine; FAME, Fatty acid methyl ester, TG triglycerides; PI, phosphatidylinositols, PE, phosphatidylethanolamine.

Figure S10. Partially assigned 600 MHz 1D NMR spectra of (**A**) aqueous liver extract and (**B**) urine from mice. Numerical keys are described in Table S4.

Figure S11. Identification of 2-ketoadipate in urine from WT female fed pesticide chow. (A) ^{1}H-^{1}H 800MHz TOCSY spectra of a representative female urine sample showing the cross-peaks between the different signals of 2-oxoadipate (multiplet at 1.84 ppm, triplet at 2.22 ppm, and triplet at 2.79 ppm). (B) A spike-in experiment was performed in a representative urine sample using the standard of 2-oxoadipate and confirmed an increase of the three above-described signals (as pointed by black arrows) in the spiked-in sample.

Figure S12. Area under the curve integrated for the 1.81-1.84 ppm (triplet) signal of 2-ketoadipate obtained from ^{1}H NMR urine samples analysis of WT female mice fed control (C) or pesticide (P) chow for 6, 36, or 48 weeks.

Figure S13. Venn diagram representing the number of hepatic genes specifically down-regulated after 52 weeks of pesticide exposure in male and female mice (n=6 mice per group). A total of 511 genes were specifically down-regulated in female mice ($p<0.05$), whereas 853 genes were significantly down-regulated in male mice. Using the David Bioinformatic ressource, different GO terms were identified in female and male mice. Histograms show the enrichment score for each pathway. Gene number and the corresponding p-value are indicated to the right of the histograms.

Figure S14. Comparison of genes identified as upregulated in response to pesticide exposure in female mice with PPARα-sensitive genes as identified from Montagner et al. (2016) and Regnier et al. (2017). (**A**) Venn diagram showing the numbers of hepatic genes specifically up-regulated in response to pesticides in female mice ($p<0.05$) in this study, the number PPARα-sensitive genes, and the number of genes shared between them. Genes were considered PPARα-sensitive when up-regulated ($p<0.05$) in response to pharmacological agonist (fenofibrate) in the liver of PPARαhep$^{+/+}$ but not in PPARαhep$^{-/-}$ mice (Montagner et al., 2016) and down-regulated ($p<0.05$) in the liver of fed PPARαhep$^{-/-}$ mice when compared to fed PPARαhep$^{+/+}$ mice (Régnier et al, 2017). (**B**) Expression profile for the 41 hepatic genes identified in our study and reported as related to PPARα – dependent pathways by Montagner et al. (2016) and Regnier et al. (2017) in females and males fed pesticide chow for 52 weeks.

Figure S15. Glucose tolerance was assessed in (**A**) male and (**B**) female CAR$^{-/-}$ mice at 16 weeks via i.p. glucose administration, at 36 and 48 weeks via oral glucose administration in the pesticide exposed (P) and control (C) groups. n=9 mice per group. Data are presented as mean ± s.e.m.

Figure S16. Kaplan-Meier survival curve for male and female WT mice fed control or pesticide chow for 52 weeks.

Table S1. Oligonucleotide sequences used in real-time PCR.

Table S2. List of the metabolites of pesticides screened by UHPL-HRMS.

Table S3. Fasting blood glucose (mg/dL) in male and female mice fed either pesticide or control chow after 16, 36, and 48 weeks.

Table S4. ^{1}H and partial ^{13}C assignments for identified metabolites. U, urine; L, liver.

Table S5. OPLS correlation coefficients determined for discriminate treatment models constructed from ^{1}H-NMR spectra for urine obtained from untreated mice and mice treated with pesticides at 6 weeks, 24 weeks, and 48 weeks. Metabolites with correlation coefficients greater than Rcrit at the 5% ($p=0.05$) level were selected as the discriminant biomarkers. A positive correlation coefficient corresponds to a relative increase in the concentration of metabolite in the pesticide-treated group and a corresponding decrease in the control group.

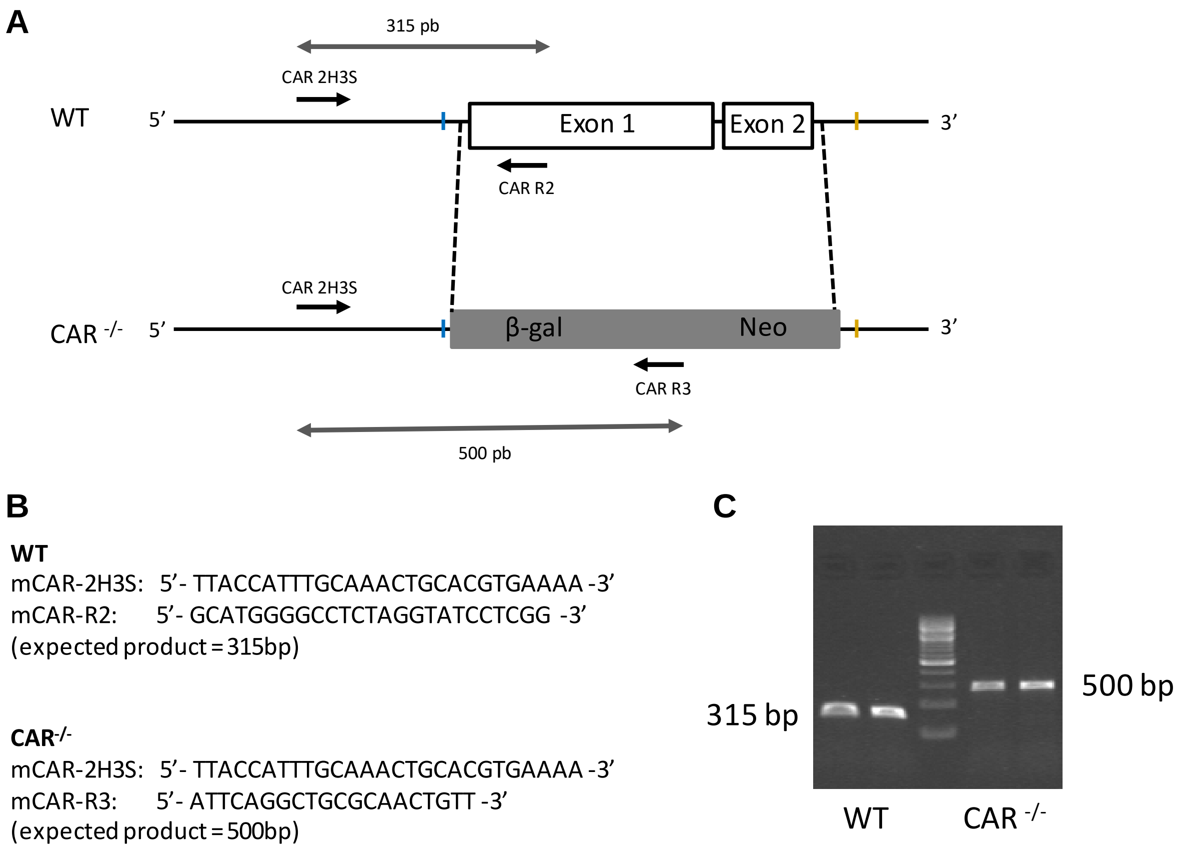

Figure S1. Diagram of the murine CAR gene. (A) Boxes represent exons 1 and 2 and arrows the foward and reverse primers CAR 2H3S and CAR R2 in WT animal, CAR 2H3S and CAR R3 in CAR$^{-/-}$ mice. Homologous recombination resulted in replacement of exon 1 and 2 with the *β-gal* and *neo* resistance genes. (B) Primer Sequences for the 5’ strand mCAR 2H3S, and for the 3’ strand mCAR R2 in WT and mCAR-R3 in CAR$^{-/-}$ animals. (C) The sizes of the generated DNA sequences using PCR were 315 and 500 bp in WT and CAR-/- mice respectively.

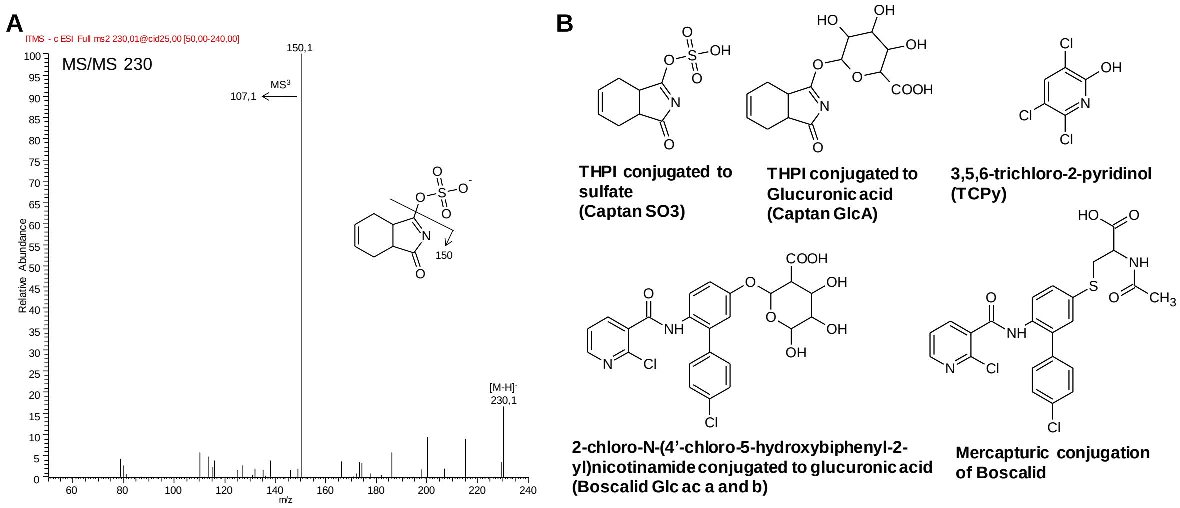

Figure S2. Pesticide metabolites identified in urine samples from male and female mice exposed for 48 weeks. (**A**) An example MS/MS spectrum of m/z 230 corresponding to [M-H] of THPI conjugated to sulphate (Captan SO3). (**B**) Chemical structures of pesticide metabolites identified in urine samples. Position of glucuronide. Boscalid Glc ac (a and b) and mercapturic conjugation of boscalid are undetermined.

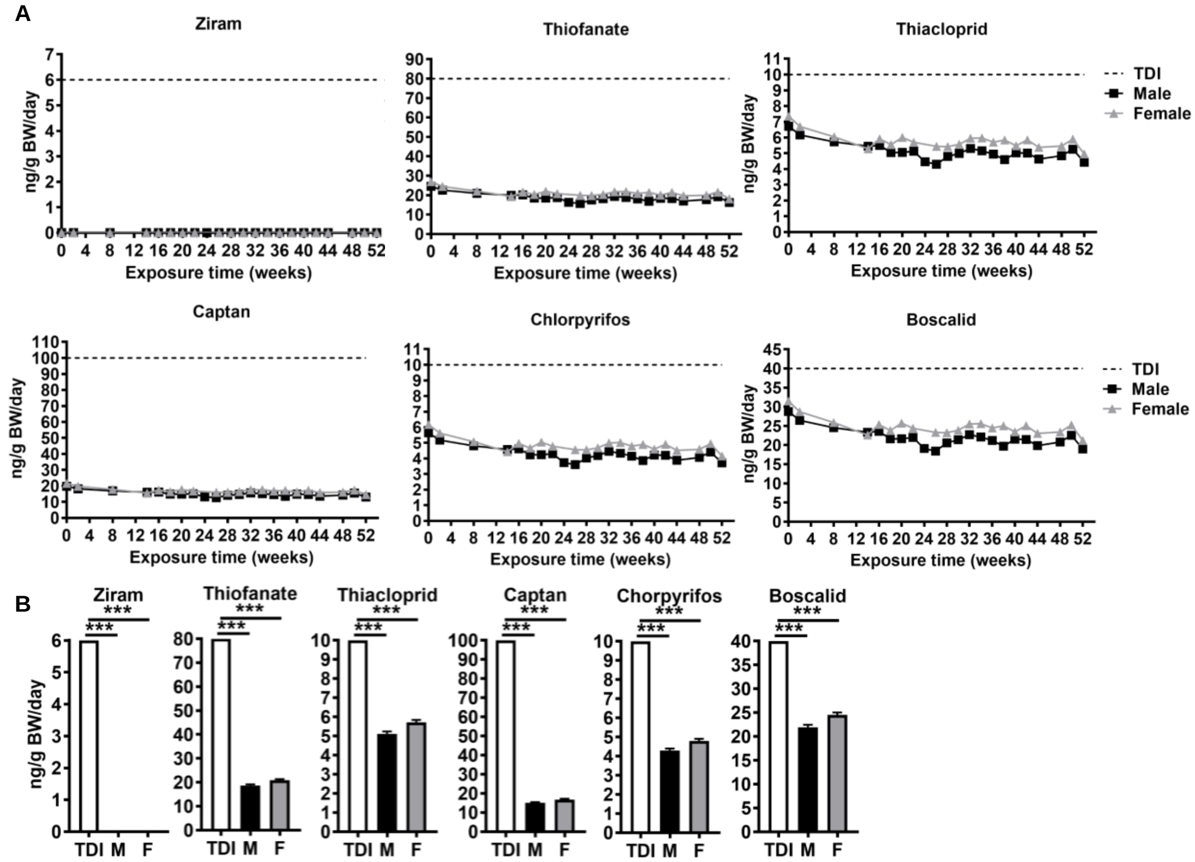

Figure S3. Quantity of ingested pesticides per gram of WT mouse. (A) Level of exposure based on pesticide levels in pellets as determined by GC/MS LC/MS/MS and measured food consumption as a function of exposure duration; (B) Mean ± standard error of the mean pesticide exposure in male (M) and female (F) mice over the 52-week exposure period. *** P<0.001 compared to respective TDI as determined using the Student's t-test. n=18 mice per group. TDI, Tolerable Daily Intake; BW body weight.

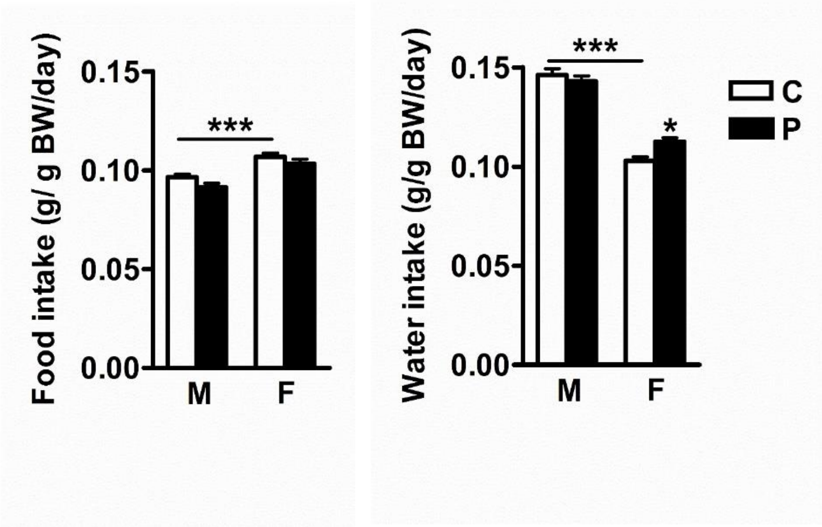

Figure S4. Food and water intake in WT male (M) and female (F) mice who were fed pesticide chow (P) or control chow (C). Data are presented as mean ± standard error of the mean. *P<0.05 compared to mice fed control chow as determined using a two-way ANOVA . ***P<0.001 between male and female mice fed control chow as determined using a two-way ANOVA.

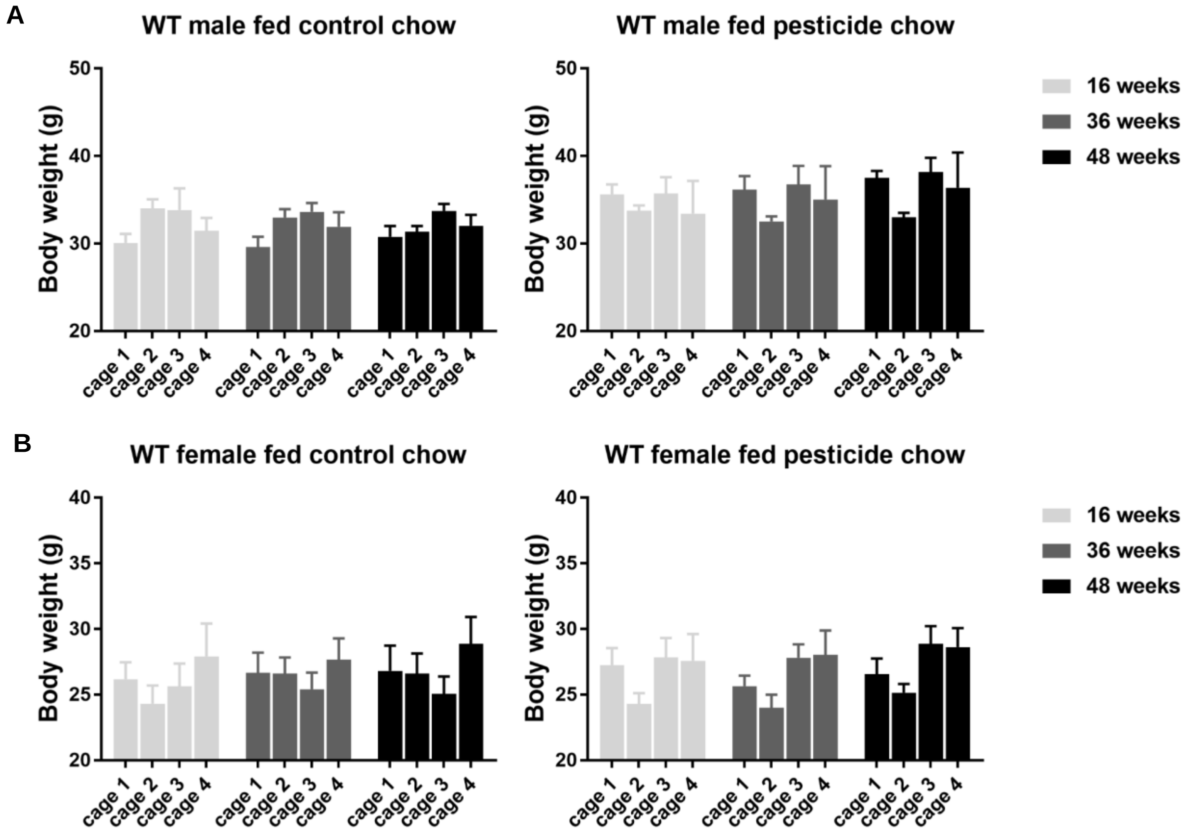

Figure S5. Body weight of WT males (**A**) fed control and pesticide chow and of females (**B**) fed control and pesticide chow after 16, 36 and 48 weeks of exposure. Results are the mean ± standard error of the mean with n=5 (cages 1 and 2) and n=4 (cages 3 and 4).

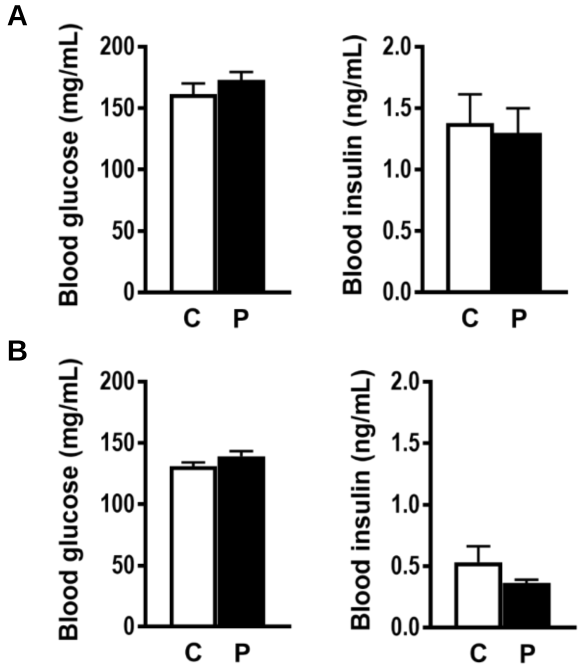

Figure S6. Blood glucose and blood insulin measured in WT male (**A**) and female (**B**) mice after 52 weeks of control (C) or pesticide (P) chow. Data are presented as mean ± standard error of the mean. n= 18 mice per group.

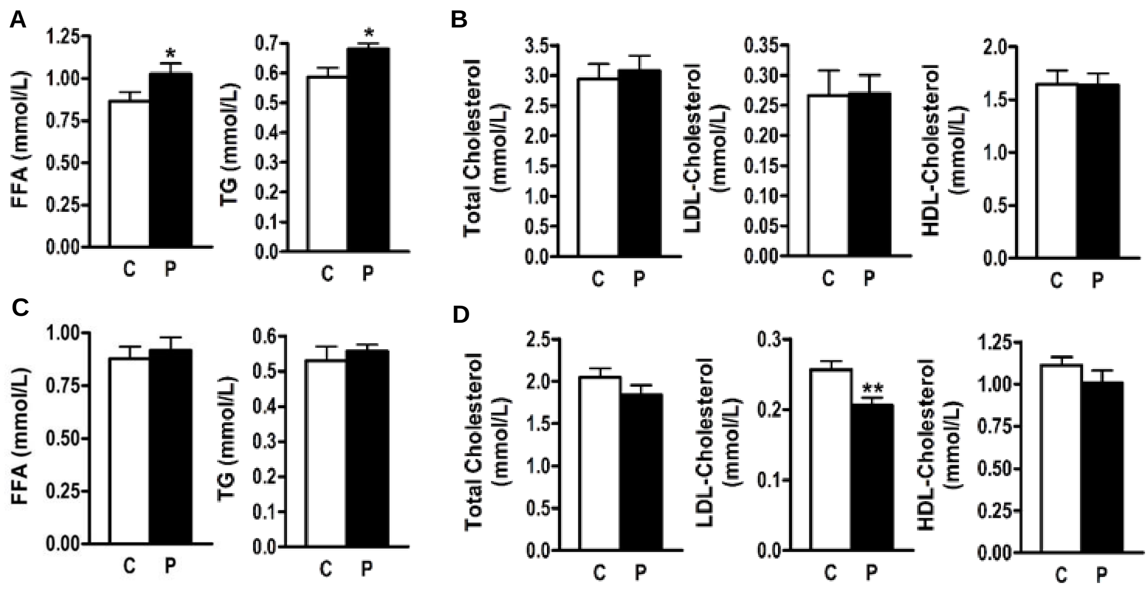

Figure S7. Analysis of plasma from WT male (**A, B**) and female (**C**, **D**) mice fed control (C) or pesticide (P) for 52 weeks. Data are presented as the mean ± standard error of the mean. *P<0.05 **P<0.01 ***P<0.001. P-values represent the difference between mice fed control chow and those fed pesticide chow as determined using a Student's t-test; n=18 mice per group. FFA, free fatty acid; TG, triglyceride; LDL, low density lipoprotein; HDL, high density lipoprotein

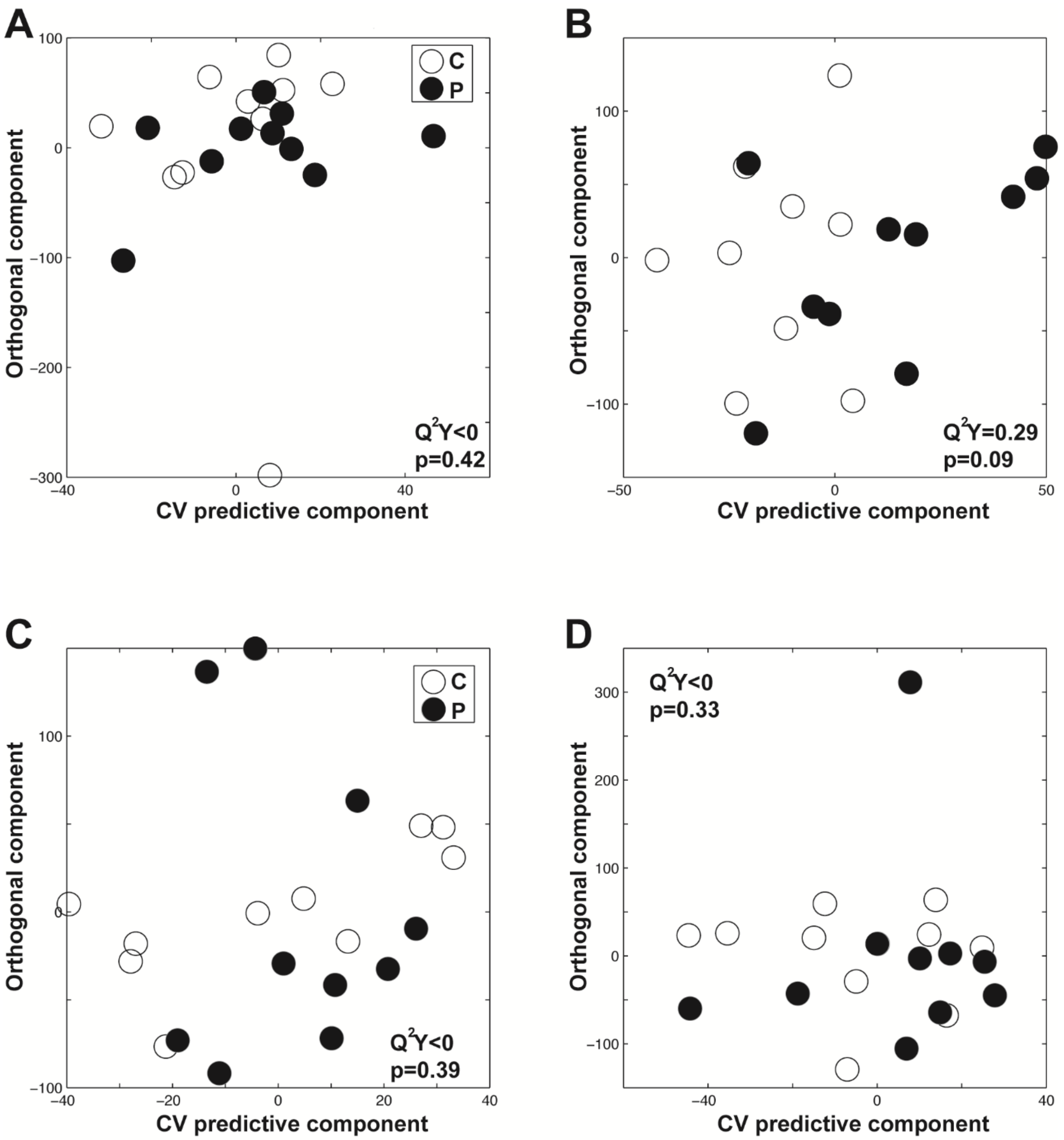

Figure S8. O-PLS-DA score plots derived from the plasma spectra of WT males (**A**), WT females (**B**), CAR-/- males (**C**) and CAR-/- females (**D**) after 48 weeks of either control (C) or pesticide (P) chow. Plasmatic biomarkers of pesticide exposure were investigated using ^{1}H-NMR based metabolomics.Q2Y represents the goodness of fit for the PLS-DA models and p-values were derived using 1000 permutations of the Y matrix.

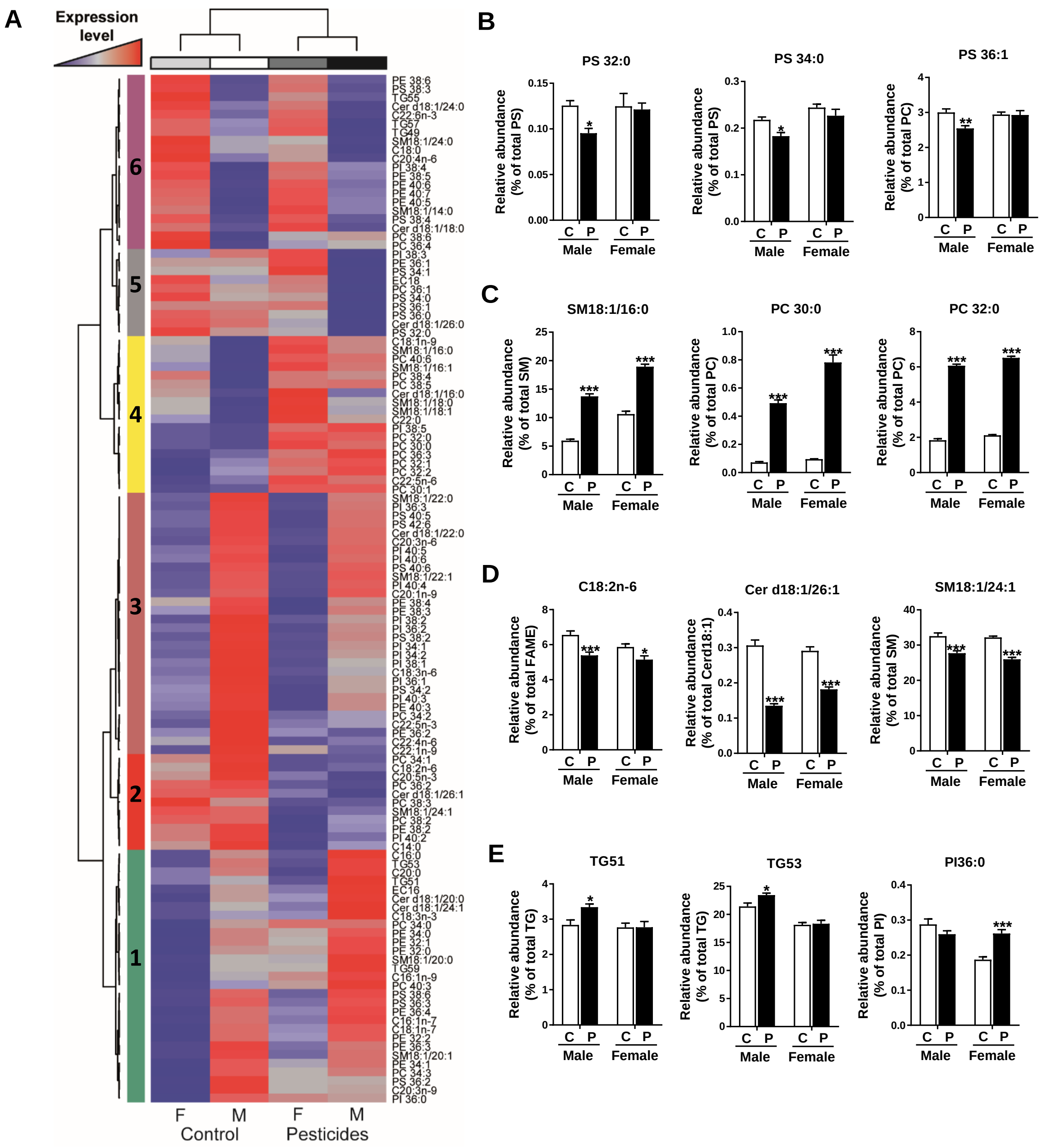

Figure S9. Hepatic lipid analysis of WT male (M) and female (F) mice after 52 weeks of eating either control (C) or pesticide (P) chow. (**A**) Heat map with hierarchical clustering, allowing the definition of 6 lipid clusters, as labeled on the left side of the map. (**B**) The relative PS32:0, PS34:0, PS36:1 abundances for cluster 5 (lipid species specifically down-regulated in males exposed to pesticides. (**C**) The relative SM18:1/16:0, PC30:0, PC 32:0 abundances for cluster 4 (lipid species up-regulated in males and females exposed to pesticides). (**D**) The relative C18:2n-6, Cerd18:1/C26:1, SM18:1/24:1 abundances for cluster 2 (lipid species down-regulated in males and females exposed to pesticides). (**E**) The relative TG51, TG53, PI36:0 abundances for cluster 1 (lipid species specifically up-regulated either in males or in females exposed to pesticides). Data are presented as the mean of relative abundance in each lipid species ± standard error of the mean. * P<0.05, ** P<0.01, *** P<0.001. P-values represent the difference between mice fed control chow and those fed pesticide chow as determined using a Student's t-test; n=18 mice per group. PS, Phosphatidylserin; SM Sphingomyelin; PC, Phosphatidlcholine; FAME, Fatty acid methyl ester, TG triglycerides; PI, phosphatidylinositols, PE, phosphatidylethanolamine.

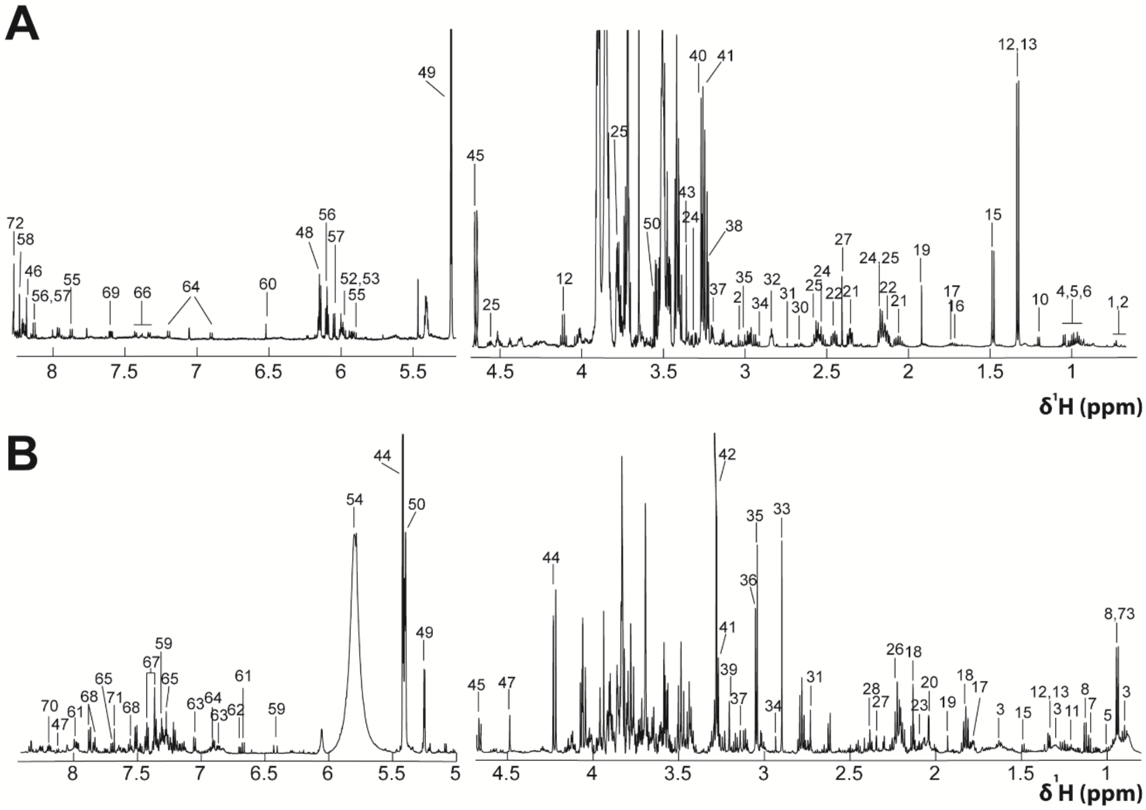

Figure S10. Partially assigned 600 MHz 1D NMR spectra of (**A**) aqueous liver extract and (**B**) urine from mice. Numerical keys are described in Table S4.

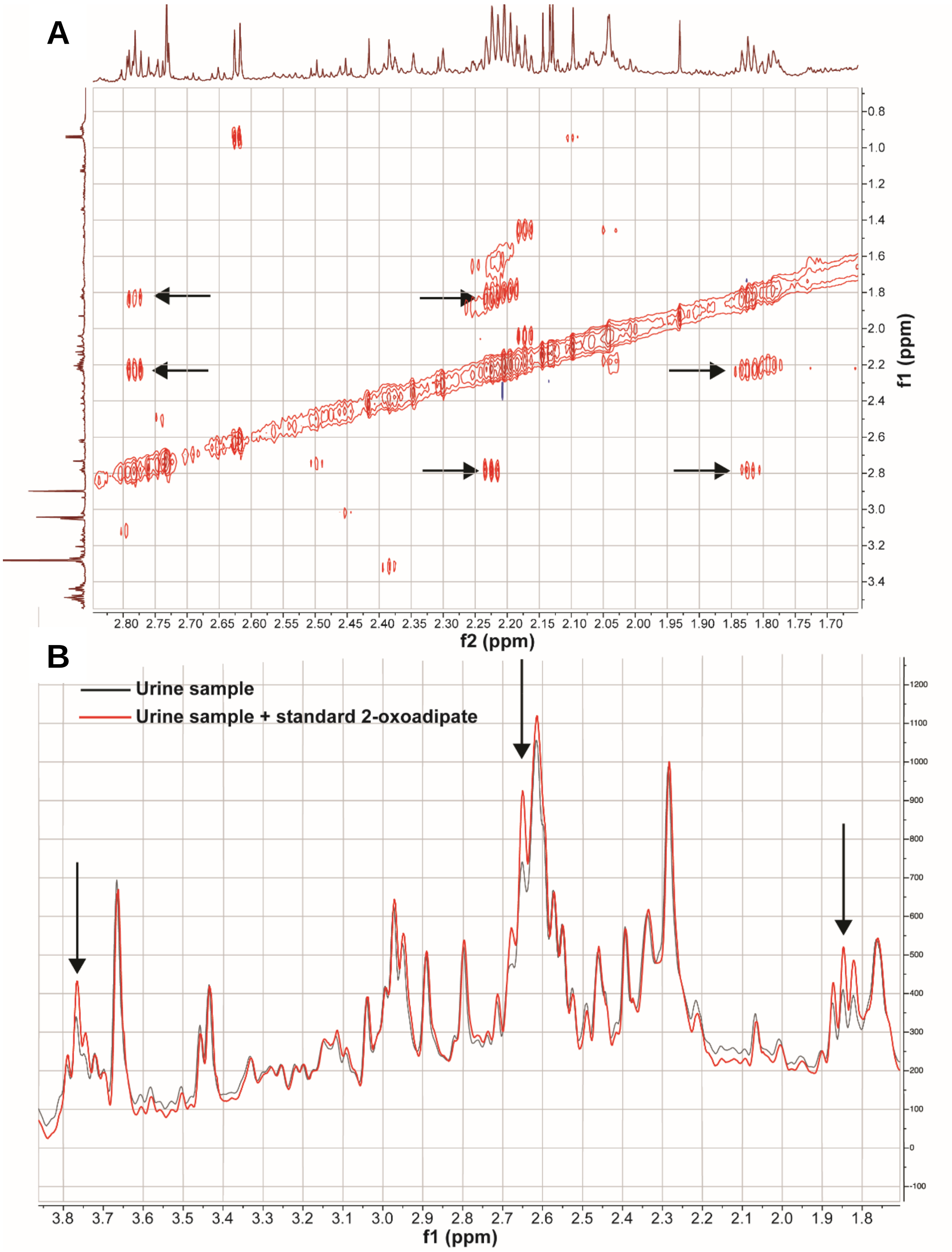

Figure S11. Identification of 2-ketoadipate in urine from WT female fed pesticide chow. (A) ^{1}H-^{1}H 800MHz TOCSY spectra of a representative female urine sample showing the cross-peaks between the different signals of 2-oxoadipate (multiplet at 1.84 ppm, triplet at 2.22 ppm, and triplet at 2.79 ppm). (B) A spike-in experiment was performed in a representative urine sample using the standard of 2-oxoadipate and confirmed an increase of the three above-described signals (as pointed by black arrows) in the spiked-in sample.

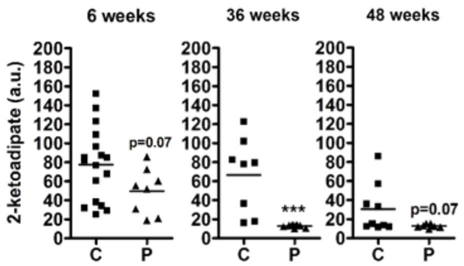

Figure S12.Area under the curve integrated for the 1.81-1.84 ppm (triplet) signal of 2-ketoadipate obtained from ^{1}H NMR urine samples analysis of WT female mice fed control (C) or pesticide (P) chow for 6, 36, or 48 weeks

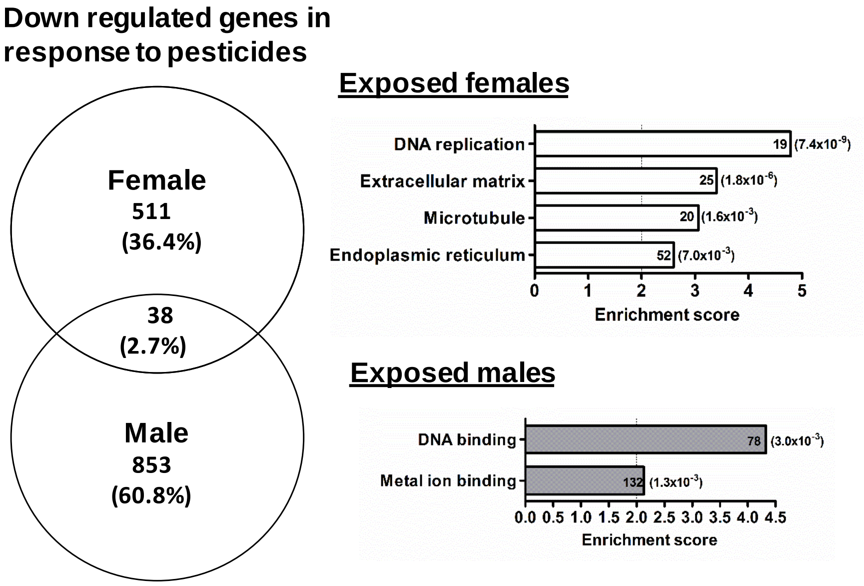

Figure S13. Venn diagram representing the number of hepatic genes specifically down-regulated after 52 weeks of pesticide exposure in male and female mice (n=6 mice per group). A total of 511 genes were specifically down-regulated in female mice ($p<0.05$), whereas 853 genes were significantly down-regulated in male mice. Using the David Bioinformatic ressource, different GO terms were identified in female and male mice. Histograms show the enrichment score for each pathway. Gene number and the corresponding p-value are indicated to the right of the histograms.

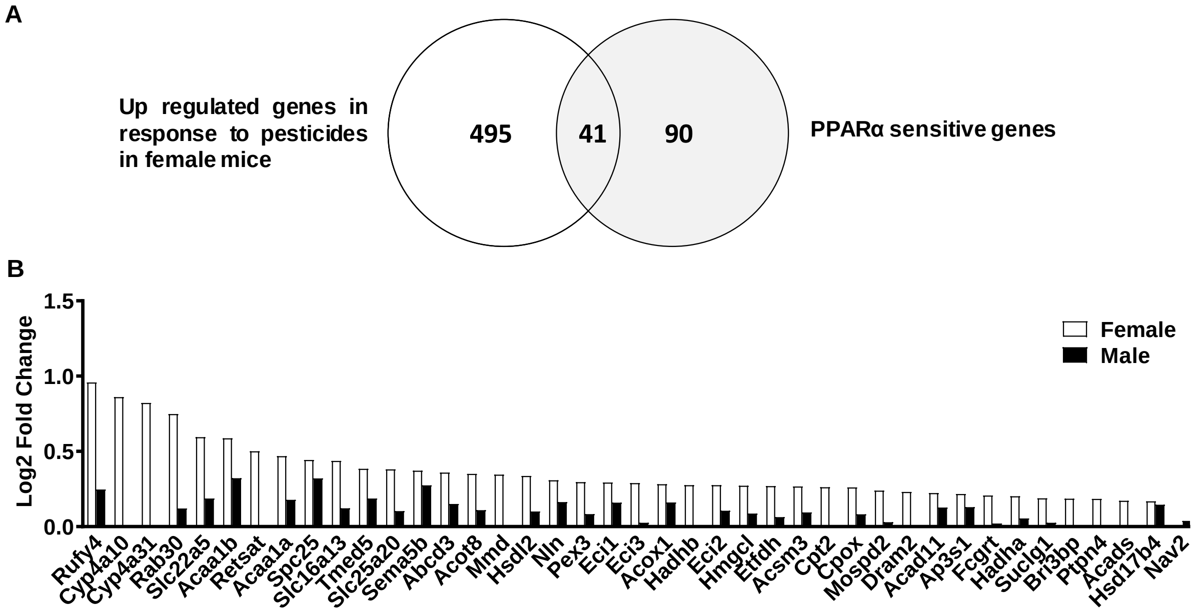

Figure S14. Comparison of genes identified as upregulated in response to pesticide exposure in female mice with PPARα-sensitive genes as identified from Montagner et al. (2016) and Regnier et al. (2017). (**A**) Venn diagram showing the numbers of hepatic genes specifically up-regulated in response to pesticides in female mice ($p<0.05$) in this study, the number PPARα-sensitive genes, and the number of genes shared between them. Genes were considered PPARα-sensitive when up-regulated ($p<0.05$) in response to pharmacological agonist (fenofibrate) in the liver of PPARαhep$^{+/+}$ but not in PPARαhep$^{-/-}$ mice (Montagner et al., 2016) and down-regulated ($p<0.05$) in the liver of fed PPARαhep$^{-/-}$ mice when compared to fed PPARαhep$^{+/+}$ mice (Régnier et al, 2017). (**B**) Expression profile for the 41 hepatic genes identified in our study and reported as related to PPARα – dependent pathways by Montagner et al. (2016) and Regnier et al. (2017) in females and males fed pesticide chow for 52 weeks.

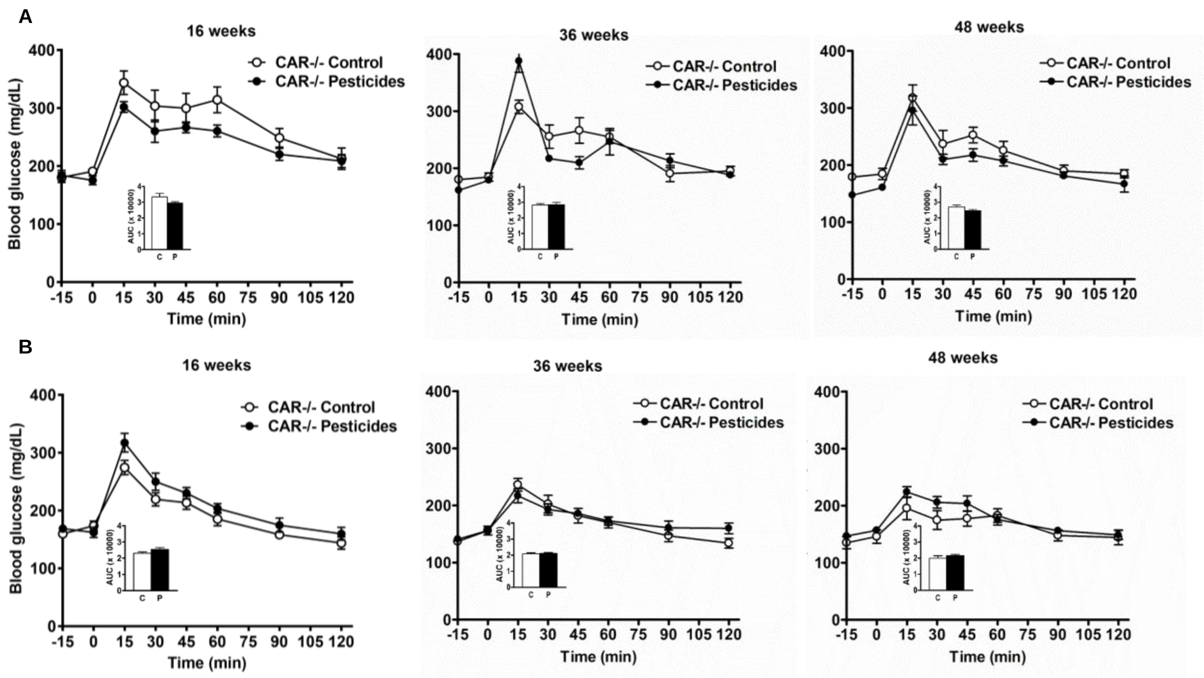

Figure S15. Glucose tolerance was assessed in (**A**) male and (**B**) female CAR$^{-/-}$ mice at 16 weeks via i.p. glucose administration, at 36 and 48 weeks via oral glucose administration in the pesticide exposed (P) and control (C) groups. n=9 mice per group. Data are presented as mean ± s.e.m.

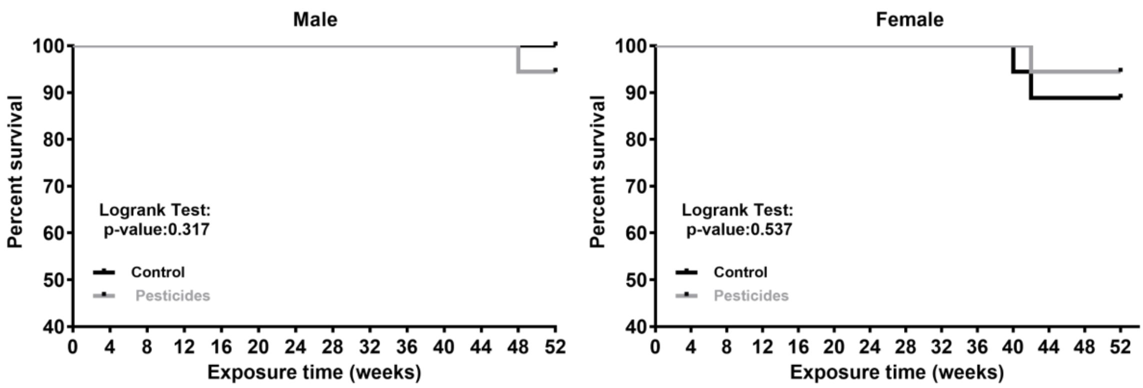

Figure S16. Kaplan-Meier survival curve for male and female WT mice fed control or pesticide chow for 52 weeks.

Table S1: Oligonucleotide sequences used in real-time PCR

Gene	NCBI Refseq	Forward primer (5'-3')	Reverse primer (5'-3')
TBP	NM_013684	ACTTCGTGCAAGAAATGCTGAA	GCAGTTGTCCGTGGCTCTCT
Cyp2b10	NM_009999	TTTCTGCCCTTCTCAACAGGAA	ATGGACGTGAAGAAAAGGAACAAC
Cyp2b9	NM_010000	CTTTGCTGGAACTGAGACCACA	GATCTGAAAATCTCTGAATCTCATGG
Cyp4a10	NM_010011	TCCAGCAGTTCCCATCACCT	TTGCTTCCCCAGAACCATCT
Ehhadh	NM_023737	CGTCTCCTCGGTTGGTGTTC	ATTATCTTCTTTGCAGTATCTAGCTGCTT
Acot5	NM_145444	CATGGCTCTGGCTTATTATAAATATGAT	CCTTTGGAAATCCCTAGCAGG
Cpt1	NM_013495	GAAGAAGAAGTTCATCCGATTCAAG	GATATCACACCCACCACCACG
Acox1	NM_015729	CAGACCCTGAAGAAATCATGTGG	CAGGAACATGCCCAAGTGAAG

Table S2. List of the metabolites of pesticides screened by UHPL-HRMS

Pesticide	Metabolite	Raw formula
Boscalid	parent	$C_{18}H_{12}Cl_2N_2O$
Boscalid	glucuronide conjugate	$C_{24}H_{20}Cl_2N_2O_7$
Boscalid	sulfate conjugate	$C_{18}H_{12}Cl_2N_2O_4S$
Boscalid	glutathione conjugate	$C_{28}H_{27}Cl_2N_5O_7S$
Boscalid	Cys-Gly conjugate	$C_{23}H_{20}Cl_2N_4O_4S$
Boscalid	mercapturate conjugate	$C_{23}H_{19}Cl_2N_3O_4S$
Boscalid	cysteine conjugate	$C_{21}H_{17}Cl_2N_3O_3S$
Boscalid	hydroxy	$C_{18}H_{12}Cl_2N_2O_2$
Boscalid	hydroxyglucuronide	$C_{24}H_{20}Cl_2N_2O_8$
Boscalid	hydroxysulfate	$C_{18}H_{12}Cl_2N_2O_5S$
Boscalid	hydroxydiglucuronide	$C_{30}H_{28}Cl_2N_2O_{14}$
Boscalid	hydroxydisulfate	$C_{24}H_{20}Cl_2N_2O_{11}S$
Boscalid	hydrolyzed	$C_6H_4NO_2Cl$
Boscalid	hydrolyzed and glucuronide conjugate	$C_{12}H_{10}NO_8Cl$
Boscalid	hydrolyzed and sulfate conjugate	$C_6H_4NO_5ClS$
Boscalid	dihydroxy	$C_{18}H_{12}Cl_2N_2O_3$
Captan	parent	$C_9H_8Cl_3NO_2S$
Captan	Glucuronide conjugate	$C_{15}H_{16}Cl_3NO_8S$
Captan	Sulfate conjugate	$C_9H_8Cl_3NO_5S_2$
Captan	THPI	$C_8H_9NO_2$
Captan	THPI glucuronide conjugate	$C_{14}H_{17}NO_8$
Captan	THPI sulfate conjugate	$C_8H_9NO_5S$
Captan	5-OH THPI	$C_8H_9NO_3$
Captan	5-OH THPI glucuronide conjugate	$C_{14}H_{17}NO_9$
Captan	5-OH THPI sulfate conjugate	$C_8H_9NO_6S$
Captan	3-OH THPI	$C_8H_9NO_3$
Captan	3-OH THPI glucuronide conjugate	$C_{14}H_{17}NO_9$
Captan	3-OH THPI sulfate conjugate	$C_8H_9NO_6S$
Captan	THPAM	$C_8H_{11}NO_3$
Captan	THPAM glucuronide conjugate	$C_{14}H_{19}NO_9$
Captan	THPAM sulfate conjugate	$C_8H_{11}NO_6S$
Captan	THPI epoxide	$C_8H_9NO_3$
Captan	THPI epoxide glucuronide conjugate	$C_{14}H_{17}NO_9$
Captan	THPI epoxide sulfate conjugate	$C_8H_9NO_6S$
Captan	5-OH THPAM	$C_8H_{11}NO_4$
Captan	5-OH THPAM glucuronide conjugate	$C_{14}H_{10}NO_{10}$
Captan	5-OH THPAM sulfate conjugate	$C_8H_{11}NO_7S$
Captan	3-OH THPAM	$C_8H_{11}NO_4$
Captan	3-OH THPAM glucuronide conjugate	$C_{14}H_{10}NO_{10}$
Captan	3-OH THPAM sulfate conjugate	$C_8H_{11}NO_7S$
Captan	diOH HHPAM	$C_8H_{11}NO_5$
Captan	diOH HHPAM glucuronide conjugate	$C_{14}H_{19}NO_{11}$
Captan	diOH HHPAM sulfate conjugate	$C_8H_{11}NO_8S$
Captan	4,5-diOH HHPI	$C_8H_{11}NO_4$
Captan	diOH HHPI glucuronide conjugate	$C_{14}H_{10}NO_{10}$
Captan	4,5-diOH HHPI sulfateconjugate	$C_8H_{11}NO_7S$
ChlorpyrifosEt	parent	$C_9H_{11}Cl_3NO_3PS$

ChlorpyrifosEt	TCPy	$C_5H_2Cl_3NO$
ChlorpyrifosEt	TCPy glucuronide conjugate	$C_{11}H_{10}Cl_3NO_7$
ChlorpyrifosEt	TCPy sulfate conjugate	$C_5H_2Cl_3NO_4S$
Thiacloprid	parent	$C_{10}H_9ClN_4S$
Thiacloprid	4-OH	$C_{10}H_9ClN_4OS$
Thiacloprid	4-OH glucuronide conjugate	$C_{16}H_{17}ClN_4O_7S$
Thiacloprid	4-OH sulfate conjugate	$C_{10}H_9ClN_4O_4S$
Thiacloprid	6-CN-glycine conjugate	$C_8H_7ClN_2O_3$
Thiacloprid	6-CN-glycine glucuronide conjugate	$C_{14}H_{15}ClN_2O_9$
Thiacloprid	6-CN-glycine sulfate conjugate	$C_8H_7ClN_4O_6S$
Thiacloprid	hydroxylamide	$C_{10}H_{11}ClN_4O_2S$
Thiacloprid	hydroxylamide glucuronide conjugate	$C_{16}H_{19}ClN_4O_8$
Thiacloprid	hydroxylamide sulfate conjugate	$C_{10}H_{11}ClN_4O_5S_2$
Thiacloprid	O-analogue	$C_{10}H_9ClN_4O$
Thiacloprid	hydrolyzed	$C_6H_4ClNO_2$
Thiacloprid	Hydrolyzed and glucuronide conjugate	$C_{12}H_{12}ClNO_8$
Thiacloprid	Hydrolyzed and sulfate conjugate	$C_6H_4ClNO_5S$
Thiophanate-Me	parent	$C_{12}H_{14}N_4O_4S_2$
Thiophanate-Me	glucuronide conjugate	$C_{18}H_{22}N_4O_{10}S_2$
Thiophanate-Me	sulfate conjugate	$C_{12}H_{14}N_4O_7S_3$
Thiophanate-Me	carbendazime	$C_9H_9N_3O_2$
Thiophanate-Me	carbendazime glucuronide conjugate	$C_{15}H_{17}N_3O_8$
Thiophanate-Me	carbendazime sulfate conjugate	$C_9H_9N_3O_5S$
Thiophanate-Me	5-OH-carbendazime	$C_9H_9N_3O_3$
Thiophanate-Me	5-OH-carbendazime glucuronide conjugate	$C_{15}H_{17}N_3O_9$
Thiophanate-Me	5-OH-carbendazime sulfate conjugate	$C_9H_9N_3O_6S$
Ziram	dithiocarbamic acid	$C_4H_8S_2$
Ziram	dithiocarbamic glucuronide conjugate	$C_{10}H_{16}O_6S_2$
Ziram	dithiocarbamic glutathione conjugate	$C_{14}H_{23}N_3O_6S_2$
Ziram	dithiocarbamic Cys-Gly conjugate	$C_9H_{16}N_2O_3S_2$
Ziram	dithiocarbamic mercapturate conjugate	$C_9H_{15}NO_3S_2$
Ziram	dithiocarbamic cysteine conjugate	$C_7H_{13}NO_2S_2$
Ziram	carbamic acid	$C_4H_8O_2$
Ziram	carbamic acid glucuronide conjugate	$C_{10}H_{16}O_8$
Ziram	carbamic acid sulfate conjugate	$C_4H_8O_5S$

Table S3. Fasting blood glucose (mg/dL) in male and female mice fed either pesticide or control chow after 16, 36, and 48 weeks.

Exposure	**Male mice**	**Female mice**	**P-value[a]**
Control chow			
16 weeks	131.5	170.1	0.001
36 weeks	124.0	142.7	0.019
48 weeks	118.1	144.3	0.035
Pesticide chow			
16 weeks	145.8	182.6	0.002
36 weeks	145.4	182.8	0.003
48 weeks	163.0	172.2	0.045

Note: n=9 mice per group.

[a]P values represent difference between male and female mice as determined using a Student's t-test.

Table S4. ^{1}H and partial ^{13}C assignments for identified metabolites. U, urine; L, liver.

Number	Metabolite	Metabolic pathway	δ ^{1}H (ppm)	Multiplicity	δ ^{13}C (ppm)	Matrix
1	Bile acids (mixed)	Bile component	**0.6-0.75**	**s**		L
			0,92	s		
2	Bile acids (tauroconjugated)	Bile component	0,72	s		L
			0,92	s		
			3,08	**t**		
3	Short and Medium Chain Fatty ac	Energy metabolism	**0,87**	**t**	16	U
			1,3	m	31,8	
			1,59	m	28,4	
			2,3	m		
4	Leucine	Amino acid	**0,96**	**t**	23,6	L
			1,72	m		
			3,74	m		
5	Valine	Amino acid metabolism	**0,99**	**d**	19,5	U, L
			1,05	**d**	**20,8**	
			2,29			
			3,62			
6	Isoleucine	Amino acid	0,94	t		L
			1,01	**d**		
			1,26	m		
			1,48	m		
			2	m		
			3,65	d		
7	α-keto-β-methyl-N-valerate	α-keto acids	0,88			
			1,1	**d**	16,5	U
			1,71			
			2,94			
8	2-ketoisocaproate	α-keto acids	0,94	d	24,6	U
			2,12			
			2,62	d	51	
9	α-ketoisovalerate	α-keto acids	1,13	d	19,3	U
			3,03	m		
10	3-hydroxybutyrate	Ketone body	**1,19**	**d**	24,4	L
			2,32	dd		
			2,4	dd		
			4,14	m		
11	β-hydroxyisovalerate	Amino acid metabolism	**1,21**	**s**	30,4	U
			2,6			
12	Lactate	Organic acids - Energy metabolism	**1,33**	**d**	22,8	U,L
			4,11	q		
13	Threonine	Amino acid metabolism	**1,33**	**d**	22,3	U,L
			3,61			
			4,23			
14	α-hydroxyisobutyrate	Amino acid metabolism	**1,36**	**s**	29,4	U
15	Alanine	Amino acid metabolism	**1,49**	**d**	19,1	U,L
			3,79			
16	Ornithine	Amino acid metabolism	**1,72**	**m**		L
			1,93	m		
			3,03	t	41,9	
			3,77	t		
17	Putrescine	Amino acid metabolism	**1,78**	**m**	25,2	U
			3,07	t		
18	2-oxoadipate	Amino acid metabolism	**1,84**	**m**	22,5	U
			2,22	t	22,5	
			2,79		41,6	
19	Acetate	Organic acids - Energy metabolism	**1,93**	**s**		U,L
20	N-acetyl groups	N-acetylated glycoproteins	**2,06**	**s**	25,2	U
21	L-glutamate	Amino acid metabolism	**2,06**	**m**	**29,8**	**L**
			2,35	m	36,4	
			3,76	dd		
22	L-glutamine	Amino acid metabolism	**2,13**	**m**	**29,3**	**L**
			2,45	m		
			3,77	t		
23	Methionine	Amino acid metabolism	**2,14**	**s**	17,15	U
			3,79			
24	Glutathion (oxidized)	Glutathion metabolism	2,17	t	29,1	L
			2,53	m	34,2	
			2,98	dd		
			3,31	m	41,6	
			3,76	m		
			4,75	**m**		
25	Glutathion (reduced)	Glutathion metabolism	2,17	m		L
			2,56	m		
			2,95	m		
			3,76	m		
			4,56	**dd**		
26	Ureidopropionate	Nucleotide metabolism	**2,38**	**t**	40,3	U
			3,31	q		

27	Succinate	Organic acids - Energy metabolism	**2,42**	**s**	36,8	U,L
28	α-ketoglutarate	Organic acids - Energy metabolism	**2,45**	**t**	33,4	U
			3,02	t		
29	Methylamine	Choline metabolism - Host-gut microbiota cometabolism	**2,61**	**s**	26,7	U
30	L-aspartic acid	Amino acid metabolism	**2,66**	**dd**		**L**
			2,8	dd		
			3,89	dd		
31	Dimethylamine	Choline metabolism - Host-gut microbiota cometabolism	**2,72**	**s**	37,6	U,L
32	Unknown 1		**2,84**	**t**	60,4	L
			3,62	m		
33	Trimethylamine	Choline metabolism - Host-gut microbiota cometabolism	**2,9**	**s**	47,6	U
34	Dimethylglycine	Choline-betaine metabolism - One carbon metabolism	**2,93**	**s**	46,5	U,L
35	Creatine	Muscle energy metabolism	**3,04**	**s**	39,9	U,L
			3,94	s	56,6	
36	Creatinine	Muscle energy metabolism - renal fonction marker	**3,05**	**s**	33,1	U
			4,07	s	59,2	
37	Choline	Choline-betaine metabolism - One carbon metabolism	**3,2**	**s**	56,7	U,L
			3,55			
38	O-phosphocholine	Choline-betaine metabolism - One carbon metabolism	**3,21**	**s**	56,6	L
			3,58	m		
			4,13	m		
39	Carnitine	Energy metabolism	**3,23**	**s**	56,8	U
40	Betaine	Amino acid metabolism	**3,27**	**s**	**55,9**	L
			3,88	s		
41	Taurine	Amino acid metabolism	3,28	t	50,4	U,L
			3,44	**t**	38,5	
42	Trimethylamine N-oxide	Choline metabolism - Host-gut microbiota cometabolism	3,28	s	62,3	U
43	Methanol		3,36	s	51,7	L
44	Sucrose	Carbohydrate metabolism	3,49			U
			3,61			
			3,7			
			5,4	**d**	95,1	
			3,81			
			4,05			
			4,23			
45	β-glucose	Carbohydrate metabolism	3,51			U,L
			3,75			
			4,66	**d**	98,7	
46	AMP		**4,01**	**dd**		L
			4,36	**dd**		
			4,5	dd		
			6,14	**d**	89,6	
			8,27	**s**		
			8,62	**s**		
47	N-methylnicotinamide	Nicotinate - nicotinamide metabolism	4,48	s	51,5	U
			8,19	t		
			8,97	d		
			9,28	s		
48	β-arabinose	Carbohydrate metabolism	3,52	d		U
			3,77			
			3,95			
			4,53	**d**		
49	α-glucose	Carbohydrate metabolism	3,45			U,L
			3,56			
			3,72			
			3,84			
			3,97			
			5,25	**d**	94,8	
50	Glycine	Amino acid metabolism	**3,56**	**s**	44,4	L
51	Allantoin	Nucleotide metabolism	**5,4**	**s**	66,2	U
52	UDP-glucose	Carbohydrate metabolism	5,6	dd		L
			5,95	d		
			7,93	**d**		
53	UDP-glucuronate	Carbohydrate metabolism	5,6	dd		L
			5,98	d		
			7,96	**d**		
54	Urea	Amino acid metabolism	**5,8**			U
55	Uridine		**5,89**	d		L
			5,9	d		
			7,89	d		

56	NADP+	Coenzyme	**6,03**	**s**		L
			6,1	d		
			8,15	**d**		
			8,42	**s**		
			8,584	**s**		
			8,82	**s**		
			9,12	**d**		
			9,3	**s**		
57	NAD+	Coenzyme	6,04	d	89,5	L
			6,09	d	102,6	
			8,18	s		
			8,2	dd		
			8,44	s		
			8,84	d		
			9,15	d		
			9,34	s		
58	Inosine	Purine metabolism	6,11	d	91,1	L
			8,23	**s**		
			8,34	s		
59	3-hydroxycinnamate	Amino acid metabolism - Host-gut microbiota cometabolism	6,43	d		U
			6,9	**dd**	118,4	
			7,16	t		
			7,31	t		
60	Fumarate	Energy metabolism	**6,52**	**s**		L
61	N-methyl-2-pyridone-5-carboxam	Nicotinate - nicotinamide metabolism	**6,67**	**d**	120,9	U
			7,96	dd	132,8	
			8,33	d	145,3	
62	N-methyl-4-pyridone-5-carboxam	Nicotinate - nicotinamide metabolism	**6,7**	**d**	122,9	U
			7,83	m		
			8,54	d		
63	p-cresol glucuronide	Amino acid metabolism - Host-gut microbiota cometabolism	6,84	d		U
			7,05	**d**	119,5	
			7,22	d		
64	Tyrosine	Amino acid metabolism	**6,87**	**d**		U,L
			7,19		132,5	
65	3-indoxylsulfate	Amino acid metabolism - Host-gut microbiota cometabolism	**7,2**	**t**		U
			7,27	t	124,3	
			7,5	**d**		
			7,7	d	120,1	
66	Phenylalanine	Amino acid metabolism	3,12	dd		L
			3,26	dd		
			7,33	**m**		
			7,38	**m**		
			7,43	m		
67	Phenylacetylglycine	Amino acid metabolism - Host-gut microbiota cometabolism	3,68	s		U
			7,36	m	131	
			7,42	**m**	131,8	
68	Hippurate	Amino acid metabolism - Host-gut microbiota cometabolism	7,56	t	135	U
			7,65	t		
			7,88	**dd**		
69	Nicotinurate	Nicotinate - nicotinamide metabolism	3,99	s		L
			7,6	**dd**		
			8,25	**m**		
			8,72	**dd**		
			8,94	**s**		
70	Nicotinamide	Nicotinate - nicotinamide metabolism	7,61	dd		U
			8,23	dd		
			8,7	**dd**		
			8,95	s		
71	Pseudouridine	Nucleotide metabolism	7,68	s	144,5	U
72	Formate	Organic acids - One-carbon metabolism	8,45	s		U,L
73	Isovalerate	Energy metabolism	0,9	d		U
			1,94	m		
			2,02	d		

Table S5. OPLS correlation coefficients determined for discriminate treatment models constructed from ^{1}H-NMR spectra for urine obtained from untreated mice and mice treated with pesticides at 6 weeks, 24 weeks, and 48 weeks. Metabolites with correlation coefficients greater than Rcrit at the 5% (p=0.05) level were selected as the discriminant biomarkers. A positive correlation coefficient corresponds to a relative increase in the concentration of metabolite in the pesticide-treated group and a corresponding decrease in the control group.

Metabolites	Metabolic class - Pathway	Diagnostic chemical shift (multiplicity)	Males			Females		
			6 weeks R2X=0.05, R2Y=0.59, Q2Y=-0.06, p=0.47	**24 weeks** R2X=0.05, R2Y=0.48, Q2Y=-0.18, p=0.52	**48 weeks** R2X=0.07, R2Y=0.99, Q2Y=0.47, p=0.14	**6 weeks** R2X=0.07, R2Y=0.62, Q2Y=0.24, p=0.04	**24 weeks** R2X=0.09, R2Y=0.79, Q2Y=0.36, p=0.03	**48 weeks** R2X=0.17, R2Y=0.98, Q2Y=0.70, p=0.001
α-keto-β-methyl-N-valerate	α-keto acids - amino acid metabolism	1.1(d)				+0.70		+0.75
α-ketoisovalerate	α-keto acids - amino acid metabolism	1.13(d)				+0.71		+0.71
Short and Medium Chain Fatty acids	Energy metabolism - Host-gut microbiota cometabolism	1.31(m)					+0.85	+0.87
N-acetylgroups	N-acetylated glycoproteins	2.04(s)						-0.79
2-ketoadipate	Amino acid metabolism	2.20 (t)					-0.89	-0.7
Trimethylamine	Choline metabolism - Host-gut microbiota cometabolism	2.89(s)						-0.77
Choline	Choline metabolism - Host-gut microbiota cometabolism	3.20(s)						-0.86
Trimethylamine-N-oxide	Choline metabolism - Host-gut microbiota cometabolism	3.27(s)						-0.81
Sucrose	Carbohydrate metabolism	4.22(d)					-0.68	-0.79
α-glucose	Carbohydrate metabolism	5.25(d)						-0.76
p-cresol glucuronide	Amino acid metabolism - Host-gut microbiota cometabolism	6.84(d)						-0.87
Phenylacetylglycine	Amino acid metabolism - Host-gut microbiota cometabolism	7.42(m)						+0.81
Pseudouridine	Nucleotide metabolism	7.68(s)						+0.70
3-indoxylsulfate	Amino acid metabolism - Host-gut microbiota cometabolism	7.5(d)						+0.74